Photocatalysis

Deutsche Ausgabe: DOI: 10.1002/ange.201412035
Internationale Ausgabe: DOI: 10.1002/anie.201412035

Activation of Water in Titanium Dioxide Photocatalysis by Formation of Surface Hydrogen Bonds: An In Situ IR Spectroscopy Study**

Hua Sheng, Hongna Zhang, Wenjing Song, Hongwei Ji, Wanhong Ma, Chuncheng Chen, and Jincai Zhao*

Abstract: *The hole-driving oxidation of titanium-coordinated water molecules on the surface of TiO_2 is both thermodynamically and kinetically unfavorable. By avoiding the direct coordinative adsorption of water molecules to the surface Ti sites, the water can be activated to realize its oxidation. When TiO_2 surface is covered by the H-bonding acceptor F, the first-layer water adsorption mode is switched from Ti coordination to a dual H-bonding adsorption on adjacent surface F sites. Detailed in situ IR spectroscopy and isotope-labeling studies reveal that the adsorbed water molecules by dual H-bonding can be oxidized to O_2 even in the absence of any electron scavengers. Combined with theoretical calculations, it is proposed that the formation of the dual H-bonding structure can not only enable the hole transfer to the water molecules thermodynamically, but also facilitate kinetically the cleavage of O–H bonds by proton-coupled electron transfer process during water oxidation.*

Photocatalytic water oxidation on TiO_2 or other metal oxide surfaces has attracted intense interest in solar energy conversion and storage[1–3] because the electrons and protons [Eq. (1)] resulting from water oxidation can be used to evolve

$$H_2O \rightarrow 1/2\,O_2 + 2\,H^+ + 2\,e^- \quad (1)$$

H_2 or reduce CO_2 for fuel production.[1,4] However, the oxidization of water to O_2 on TiO_2 surface has been proven to be quite difficult, which leaves ample opportunity for electron–hole recombination.[5–7] Actually, almost all the reported photocatalytic water oxidation reactions on the TiO_2 surface required the assistance of positive bias voltage or the consumption of electrons by oxidative sacrifice agents (that is, Ag^+, Fe^{3+}, or Ce^{4+}).[8–10] Consequently, water oxidation is regarded as the bottleneck for further improving the efficiency of solar-fuel systems.

Conventionally, the water oxidation on TiO_2 has been considered to be initiated from trapping of the photogenerated holes by molecular water or OH^- adsorbed onto the surface Ti sites (for example, the five-coordinated surface Ti atoms, Ti_{5c}) to generate $^{\bullet}OH$ radicals. The coupling of such $^{\bullet}OH$ radicals generates H_2O_2, which is further oxidized to O_2 by holes.[11,12] However, recent experimental and theoretical studies suggest that the occupied states of the O 2p orbitals of these adsorbed water species (both molecular water and OH^-) are well below the top edge of the valence band of TiO_2; therefore, the transfer of the photogenerated holes to these species is thermodynamically hindered.[13–15]

In the coordinative absorption mode of water, the donation of unpaired electrons from the oxygen atom of water to the Ti atom would greatly decrease the electron density of the oxygen atom. This should be the main reason for the thermodynamic ineffectiveness of hole transfer toward water species. Kinetically, recent theoretical calculations predicted that the oxidative cleavage of the first O–H bond, typically by the proton-coupled electron transfer process, is the rate-limiting step for the whole four-hole water oxidation reaction on TiO_2 surface.[16,17] Inspired by these, herein we developed a strategy to realize water oxidation through controlling the interaction mode between water and the photocatalyst surface sites by deliberate surface fluorination of TiO_2. Our in situ FTIR measurements and theoretical calculations showed that, by avoiding the direct coordination of water molecules on fluorinated surface and forming H-bond between the first-layer water molecules and surface F, the hole transfer to the water molecules became favorable thermodynamically and kinetically. This study highlights the essential role of the hydrogen-bond network in the photocatalytic water oxidation.

To change the interaction of water with TiO_2 surface, TiO_2 (commercially available P25, containing about 80% anatase and 20% rutile) was treated with NaF aqueous solutions with different concentrations at pH 3.5. The combined analysis on F 1s XPS and FTIR spectra (Supporting Information, Figure S1 and the detailed discussion therein) shows that the surface structure of fluorinated samples is dependent significantly on the NaF concentrations. For the sample treated with a low NaF concentration (0.02 M, denoted as F0.02), most of the surface fivefold-coordinated Ti atoms were covered by terminal F_t, but surface bridging oxygen (O_{br}) left intact (Scheme 1b).[18] After treated with increased NaF concetrations (0.1, 0.3, and 0.5 M, denoted as F0.1, F0.3, and F0.5, respectively), O_{br} was also substituted gradually by F^- (F_{br} in Scheme 1c). After F0.5 was washed with a dilute NaOH

[*] Dr. H. Sheng, H. Zhang, Dr. W. Song, Dr. H. Ji, Prof. W. Ma, Prof. C. Chen, Prof. J. Zhao
Key Laboratory of Photochemistry
National Laboratory for Molecular Sciences, Institute of Chemistry
Chinese Academy of Sciences, Beijing 100190 (China)
E-mail: ccchen@iccas.ac.cn

[**] We appreciate the financial support by the 973 project (2010CB933503, 2013CB632405), the NSFC (No. 21137004, 21221002, 21227011, and 21277147), and the "Strategic Priority Research Program " of the Chinese Academy of Sciences (No. XDA09030200).

Supporting information for this article is available on the WWW under http://dx.doi.org/10.1002/anie.201412035.

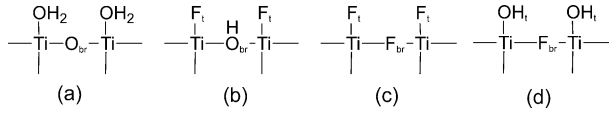

Scheme 1. The surface structures of a) pristine TiO_2 and b)–d) TiO_2 with different fluorination configurations.

solution (sample F0.5b), the terminal F_t was replaced by OH_t, while F_{br} is resistant to the washing (Scheme 1 d).[19]

The photochemical activities of pristine and fluorinated samples were examined by in situ FTIR spectroscopy. As shown in Figure 1 a, in the absence of any redox species except water, UV irradiation caused no obvious change in the

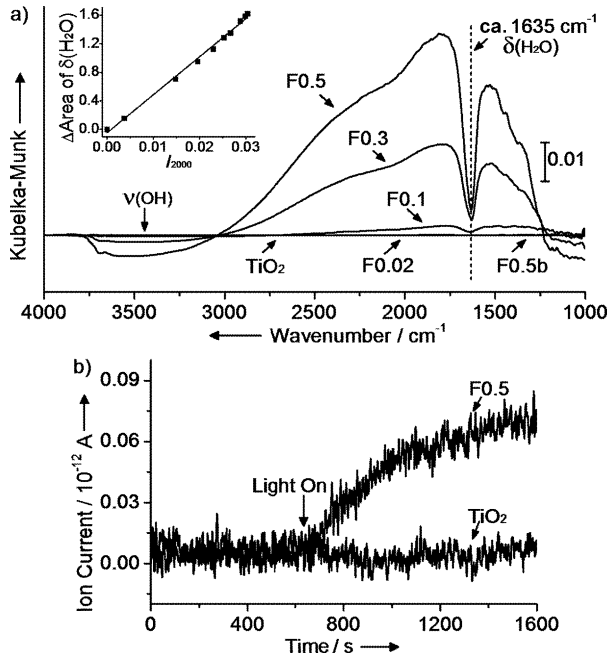

Figure 1. a) Change in IR spectra of different TiO_2 samples (pretreated by outgassing at 298 K, with similar amounts of surface adsorbed water left; Supporting Information, Figure S2) after 20 min UV irradiation under 1 atm Ar. Inset: linear relationship between the area of the negative peak at about 1635 cm^{-1} ($\delta(H_2O)$) and absorbance at 2000 cm^{-1} (I_{2000}) on the F0.5 surface. b) Time course of the generation of $^{18}O_2$ detected by mass spectra. The samples (F0.5 and TiO_2) were dispersed in $H_2{}^{18}O$.

IR spectra of the pristine TiO_2 and F0.02. Intriguingly, in the cases of F0.1, F0.3, and F0.5, the UV irradiation induced an evident increase in a monotonic IR absorption band ranging from 3000 to 1000 cm^{-1}, which is attributed to the accumulated conduction-band electrons (e_{cb}^-).[20,21] Furthermore, this featureless absorption band became more pronounced as the extent of fluorination increased. Concomitant with the e_{cb}^- accumulation, considerable surface-adsorbed water molecules were lost, as indicated by the appearance of the negative broad absorption band ranging from 3700 to 3000 cm^{-1} and the negative peak at about 1635 cm^{-1}, assigned to ν(OH) and $\delta(H_2O)$, respectively. However, when F0.5 was washed with a dilute alkaline solution (sample F0.5b), neither the accumulation of e_{cb}^- nor the loss of water molecules was observed any more.

The increase of the e_{cb}^- accumulation (represented by the IR intensity at 2000 cm^{-1}, I_{2000}) exhibited an excellent linear relationship with the loss of the adsorbed molecular water (represented by the area of the negative peak at about 1635 cm^{-1}) as shown in the inset of Figure 1 a. Furthermore, with the introduction of O_2 (Supporting Information, Figure S3b) and the stop of UV irradiation (Supporting Information, Figure S3c), a dramatic decrease in e_{cb}^- accumulation occurred simultaneously with a recovery of water, owing to the reaction between accumulated e_{cb}^- and O_2 regaining water [Eq. (2)]. The almost identical variation trends of e_{cb}^-

$$1/2\,O_2 + 2\,e_{cb}^- + 2\,H^+ \rightarrow H_2O \qquad (2)$$

accumulation and the decrease of adsorbed water under all tested conditions (Supporting Information, Figure S3d) exclude the possibility that the loss of the adsorbed water during the photoreaction was merely physical desorption and confirm that the accumulation and depletion of e_{cb}^- are the results of the water oxidation [Eq. (1)] and O_2 reduction [Eq. (2)], respectively. Another strong support for the occurrence of water oxidation came from the observations that e_{cb}^- accumulation was markedly increased in the water-saturated atmosphere (Supporting Information, Figure S4).

The photoreactions were further monitored by isotope-labeled mass spectrometry to verify the oxidation of water to O_2 on F0.5. In this measurement, pristine TiO_2 and F0.5 were dispersed in $H_2{}^{18}O$ to exclude the possible inference of $^{16}O_2$ in air. Under irradiation by a 300 W xenon lamp, as shown in Figure 1 b, the signal for $^{18}O_2$ ($m/z = 36$) gradually increased in the F0.5 dispersion, whereas the signal for $^{18}O_2$ in the pristine TiO_2 system was not detectable, irrespective of the irradiation. These experimental observations confirm that the molecular oxygen, O_2, on F0.5 evolves from water under UV irradiation.

By exposing the dehydrated F0.5 to Ar flow saturated with a H_2O/D_2O (1:1, v/v) mixture, three water species of H_2O, HDO, and D_2O with bending absorption at 1635, 1445, and 1212 cm^{-1}, respectively, were observed (Supporting Information, Figure S5). During UV irradiation, as shown in Figure 2, all the three bending absorption peaks underwent a significant decrease, concomitant with e_{cb}^- accumulation. When estimating the relative loss rates of the three bending absorption peaks, pseudo-zero-order kinetics were observed for all three peaks, with apparent rate constants of 0.046 (k_{H_2O}), 0.025 (k_{HDO}), and 0.012 (k_{D_2O}). A deuterium kinetic isotope effect (k_{H_2O}/k_{D_2O}) of 3.8 indicates that the breakage of an O–H bond in the water molecules during the photoreaction is the rate-determining step for the loss of water, which is in agreement with earlier theoretical predictions.[16,17] Therefore, the possibility of the oxidation of the lattice O of TiO_2 to O_2 can be excluded because of the rate-determining step of O–H bond cleavage rather than Ti–O bond. Thus, considering all these results, we concluded that the dominant contribution in e_{cb}^- accumulation on F0.5 is from the oxidation of water to O_2.

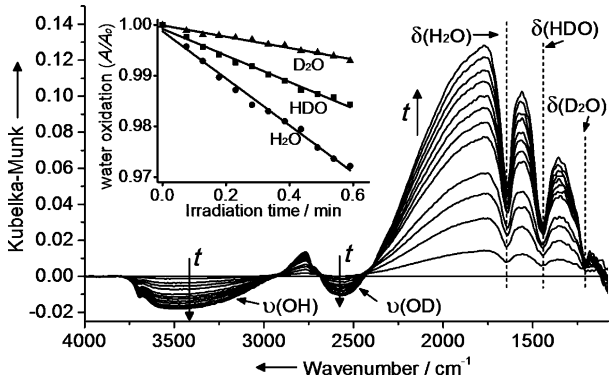

Figure 2. Change in IR spectra during the photocatalytic oxidation of a 1:1 mixture of H_2O and D_2O on F0.5 under UV irradiation. Inset: kinetics of the decrease in the area of the $\delta(H_2O)$, δ(HDO), and $\delta(D_2O)$ bands upon UV irradiation under an Ar atmosphere.

To reveal the relationship between the activity and adsorption modes of water molecules, we compared the IR spectra of pristine TiO_2 and F0.5 when being dehydrated at different temperatures (298–623 K, Figure 3a). IR absorptions of water molecules on pristine TiO_2 completely dis-

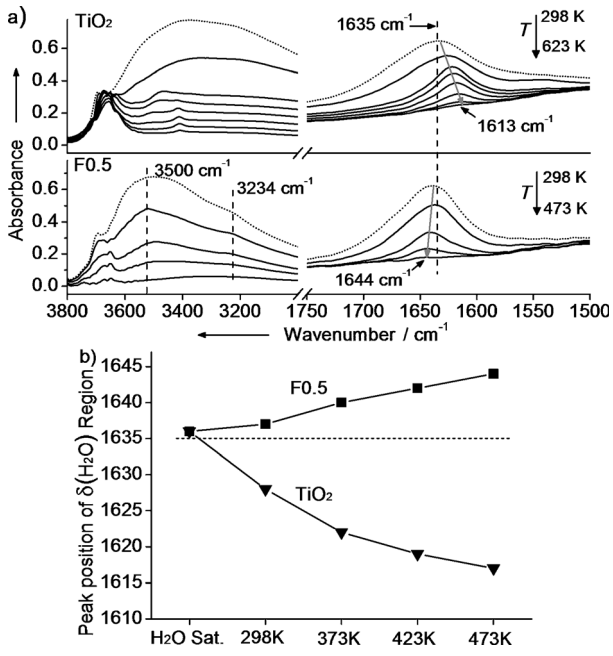

Figure 3. a) IR spectra (ν(OH) and $\delta(H_2O)$ regions) of TiO_2 and F0.5 under conditions of water saturation (•••••) or dehydration at different temperatures (TiO_2: 298–623 K, F0.5: 298–473 K, 50 K interval for the adjacent dehydration temperatures). The background was collected on dry KBr. b) The wavenumbers at peak maxima of $\delta(H_2O)$ as a function of the outgassing temperature (298–473 K) for TiO_2 and F0.5.

appeared at 623 K, whereas that on F0.5 was achieved at merely 473 K, suggesting a much weaker interaction of water molecules with F0.5 surface. Interestingly, the change trend in IR absorption of $\delta(H_2O)$ region for F0.5 was entirely different from that for pristine TiO_2. In the case of pristine TiO_2, the peak maxima of this vibration were remarkably shifted to a lower wavenumber (from ca. 1635 to ca. 1613 cm^{-1}) during the dehydration, whereas the wavenumbers in the spectrum of F0.5 increased slightly from about 1635 to about 1644 cm^{-1} (Figure 3b). Furthermore, the absorption maxima of ν(OH) vibration exhibited a significant red-shift with the increased water adsorption on pristine TiO_2. However, on F0.5, absorption maxima were located around 3500 cm^{-1} and did not undergo obvious shift with the increase of water coverage. In the rehydration processes of the dehydrated TiO_2 samples, similar IR behaviors with respect to the extent of hydration were observed (Supporting Information, Figure S6). All these indicate the unique hydrogen-bonding network of F0.5-adsorbed water molecules.

For TiO_2, it is generally accepted that the water molecules are adsorbed molecularly on the Ti_{5c} sites in the first layer, and the outer layer of water molecules are then attached to the inner layer by H-bonds to form a network structure around the TiO_2 surface.[22,23] The cross-linking H-bond structure was reported to blue-shift the bending vibration of H_2O, and the extent of this shift increase with increasing numbers of H-bonds.[24] Accordingly, the shifts in the IR absorption of the $\delta(H_2O)$ and ν(OH) regions during the hydration and dehydration (Figure 3; Supporting Information, Figure S6) reflect the gradual formation and cleavage of the H-bond network, respectively. Unlike the case of pristine TiO_2, the vibration of $\delta(H_2O)$ for F0.5 emerges at a relatively large wavenumber (1644 cm^{-1}) and a remarkably red-shifted ν(OH) absorption band at 3234 cm^{-1} was observed, even when the amount of adsorbed water is very low, which suggests that the H-bond is formed in the first-layer adsorption of H_2O onto F0.5. Fluoride ions are known to form strong H-bonds with molecular H_2O. Our XPS and IR results (Supporting Information, Figure S1) demonstrate convincingly that fluorides F_{br} and F_t in F0.5 tend to exist in pairs and coordinate to the same Ti sites (Scheme 1c). Therefore, the two H atoms of water likely interact simultaneously with the adjacent F_t and F_{br} through dual H-bonds (Scheme 2b). The

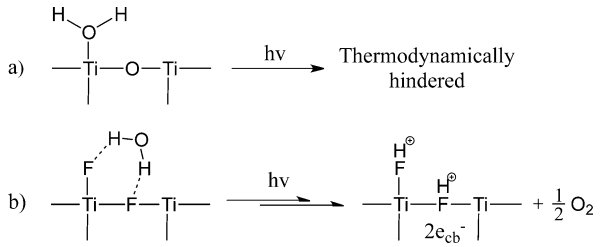

Scheme 2. Pathways of water oxidation under different water adsorption configurations.

formation of dual H-bonds would reinforce the intrinsic bending force constant, subsequently leading to a higher vibration frequency of $\delta(H_2O)$.[24] This supposition is also supported by fact that the change tendencies in both the ν(OH) and $\delta(H_2O)$ regions on either F0.02 or F0.5b are similar with those on pristine TiO_2 (Supporting Information, Figure S7).

To estimate the energetics for the oxidation of water with different adsorption modes by the hole, the density of states

and the hole-distribution were examined by density functional theory (DFT) calculations on the anatase (101) slab. We considered two adsorption modes of water: 1) a water molecule adsorbed onto F sites by dual H-bonding to adjacent F_t and F_{br}, and 2) water adsorbed onto five-fold-coordinated Ti (Ti_{5c}) sites of TiO_2 through its oxygen atom in the first layer, as shown in Figure 4a. The DFT study with hybrid functional (PBE0) showed that the partial density of states

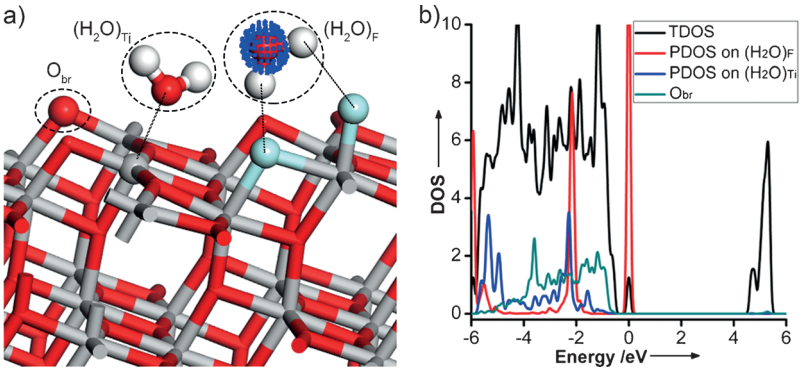

Figure 4. a) Spin-density contour (blue dots) for the fluorinated (101) slab of anatase TiO_2 with one extra hole. Two adsorption modes for water molecules, $(H_2O)_F$ and $(H_2O)_{Ti}$, are compared on the same surface. b) The total density of states (TDOS) and partial density of states (PDOS) on different oxygen atoms. Ti gray, O red, F cyan, H white.

(PDOS) of $(H_2O)_{Ti}$ was deeply embedded in the valence band by approximately 2 eV, which is consistent with previous reports that the occupied states of O 2p orbitals of Ti-adsorbed water species are well below the top edge of the valence band of TiO_2.[13–15] Notably, the PDOS on the H-bonding adsorbed water $(H_2O)_F$ was located just above the top of the valence band, which is mainly derived from the O 2p orbital of the O atom in TiO_2 (Figure 4b), indicating that it is energetically favorable for the hole trapping by the water molecules adsorbed onto F by H-bonds. In good agreement with the DOS results, the spin distribution analysis of the slab with an extra hole reveals that large spin densities (blue dots) are localized on the oxygen atom of the H-binding adsorbed water molecule, $(H_2O)_F$, whereas no hole-distribution is observed on the Ti-coordinated water, $(H_2O)_{Ti}$ (Figure 4a). The presence of second layer water molecules to form hydrogen bonds with $(H_2O)_{Ti}$ does not change the relative energy profiles of the first-layer water molecules (Supporting Information, Figure S8).

Evidently, the alteration of the water adsorption mode on TiO_2 by surface fluorination can significantly influence the thermodynamics and kinetics of water oxidation by the hole. In the case of pristine TiO_2, the Mulliken charge on the O atom in water coordinated to the Ti_{5c} sites is −0.94. However, the charge on the O atom of water that adsorbs by H-bonding to surface F atoms is −1.06, which is much more negative than that of water coordinated to Ti_{5c} sites. Plausibly, the hydrogen in water as an H-bond donor will weaken its H—O bonds and leave a more negative charge on the O atom. As a result, the formation of this H-bond will make the hole trapping by the O atom energetically more favorable.

According to the theoretical calculation results, in the cases of samples containing both F_t and F_{br}, such as F0.1, F0.3, and F0.5, the water was bonded to the surface via dual H-bonding with neighboring F_t and F_{br} (Scheme 2b). First, through dual H-bonding, the proton transfer between the catalyst and adsorbed water molecules will be strengthened. According to the observed remarkable KIE (Figure 2) and recent reports,[16,17,25] this facilitation in proton transfer will significantly enhance the water oxidation. Second, The presence of F^- in TiO_2 aqueous suspensions, where only surface Ti sites was covered by terminal F_t, has been reported to promote the degradation of organic pollutants and to enhance the formation of ·OH radicals.[12,26,27] Under our experimental conditions, neither electron accumulation nor water oxidation was observed for the sample covered only by F_t, as in F0.02, probably because of the prevalence of recombination between the ·OH radicals and e_{cb}^- in the absence of scavenger. The lack of photocatalytic activity of F0.02 suggests the multi-hole oxidation characteristics of the dual H-bonding absorbed water molecules on F0.5. It is proposed that with both H atoms of water molecule H-bonding with surface F sites, the formed radical intermediates by hole transfer are restricted on the surface through H-bonds, which enables multi-hole oxidation of water oxidize into O_2; this process should be accompanied by the breakage of O—H and the nucleophilic attack of water in the outer layer or the coupling of two oxidized water molecules.

In conclusion, on the basis of a detailed in situ IR investigation, we show that, through the alteration of the water adsorption mode on TiO_2 by surface fluorination, photocatalytic water oxidation to dioxygen by photogenerated holes was achieved in the absence of any electron scavengers, which is attributed to the assistance of surface H-bonding formed between the water molecules and two adjacent surface F sites. Such a H-bonding water adsorption configuration can not only facilitate proton transfer and cleavage of O—H bonds in water molecules but also enable the hole transfer from the valence band to the water molecules, which is energetically unfavorable in the case of Ti_{5c}-adsorbed water molecules.

Keywords: hydrogen bonds · IR spectroscopy · photocatalysis · titanium dioxide · water oxidation

How to cite: *Angew. Chem. Int. Ed.* **2015**, *54*, 5905–5909
Angew. Chem. **2015**, *127*, 6003–6007

[1] W. J. Youngblood, S. H. A. Lee, K. Maeda, T. E. Mallouk, *Acc. Chem. Res.* **2009**, *42*, 1966–1973.
[2] Y. Q. Qu, X. F. Duan, *Chem. Soc. Rev.* **2013**, *42*, 2568–2580.
[3] M. Woodhouse, B. A. Parkinson, *Chem. Soc. Rev.* **2009**, *38*, 197–210.
[4] D. Gust, T. A. Moore, A. L. Moore, *Acc. Chem. Res.* **2009**, *42*, 1890–1898.
[5] M. Yagi, M. Kaneko, *Chem. Rev.* **2001**, *101*, 21–35.

[6] J. W. Tang, J. R. Durrant, D. R. Klug, *J. Am. Chem. Soc.* **2008**, *130*, 13885 – 13891.
[7] Q. Guo, C. B. Xu, Z. F. Ren, W. S. Yang, Z. B. Ma, D. X. Dai, H. J. Fan, T. K. Minton, X. M. Yang, *J. Am. Chem. Soc.* **2012**, *134*, 13366 – 13373.
[8] A. Fujishima, X. T. Zhang, D. A. Tryk, *Surf. Sci. Rep.* **2008**, *63*, 515 – 582.
[9] X. B. Chen, S. S. Mao, *Chem. Rev.* **2007**, *107*, 2891 – 2959.
[10] M. G. Walter, E. L. Warren, J. R. McKone, S. W. Boettcher, Q. X. Mi, E. A. Santori, N. S. Lewis, *Chem. Rev.* **2010**, *110*, 6446 – 6473.
[11] D. W. Bahnemann, M. Hilgendorff, R. Memming, *J. Phys. Chem. B* **1997**, *101*, 4265 – 4275.
[12] C. Minero, G. Mariella, V. Maurino, E. Pelizzetti, *Langmuir* **2000**, *16*, 2632 – 2641.
[13] M. A. Henderson, *Surf. Sci. Rep.* **2002**, *46*, 1 – 308.
[14] P. Salvador, *J. Phys. Chem. C* **2007**, *111*, 17038 – 17043.
[15] R. Nakamura, Y. Nakato, *J. Am. Chem. Soc.* **2004**, *126*, 1290 – 1298.
[16] J. Chen, Y. F. Li, P. Sit, A. Selloni, *J. Am. Chem. Soc.* **2013**, *135*, 18774 – 18777.
[17] A. Valdés, G. J. Kroes, *J. Phys. Chem. C* **2010**, *114*, 1701 – 1708.
[18] M. Minella, M. G. Faga, V. Maurino, C. Minero, E. Pelizzetti, S. Coluccia, G. Martra, *Langmuir* **2010**, *26*, 2521 – 2527.
[19] Q. Wang, C. C. Chen, D. Zhao, W. H. Ma, J. C. Zhao, *Langmuir* **2008**, *24*, 7338 – 7345.
[20] D. A. Panayotov, S. P. Burrows, J. R. Morris, *J. Phys. Chem. C* **2012**, *116*, 4535 – 4544.
[21] F. Guzman, S. S. C. Chuang, *J. Am. Chem. Soc.* **2010**, *132*, 1502 – 1503.
[22] M. Sumita, C. P. Hu, Y. Tateyama, *J. Phys. Chem. C* **2010**, *114*, 18529 – 18537.
[23] A. Tilocca, A. Selloni, *Langmuir* **2004**, *20*, 8379 – 8384.
[24] G. van der Rest, M. Masella, *J. Mol. Spectrosc.* **1999**, *196*, 146 – 148.
[25] J. Cheng, X. D. Liu, J. A. Kattirtzi, J. Vande Vondele, M. Sprik, *Angew. Chem. Int. Ed.* **2014**, *53*, 12046 – 12050; *Angew. Chem.* **2014**, *126*, 12242 – 12246.
[26] J. S. Park, W. Choi, *Langmuir* **2004**, *20*, 11523 – 11527.
[27] H. Sheng, Q. Li, W. H. Ma, H. W. Ji, C. C. Chen, J. C. Zhao, *Appl. Catal. B* **2013**, *138*, 212 – 218.

Received: December 15, 2014
Revised: March 2, 2015
Published online: March 25, 2015

